J|A|C|S
COMMUNICATIONS

Published on Web 07/01/2006

Controlled Synthesis and Self-Assembly of CeO_2 Nanocubes

Songwang Yang and Lian Gao*

State Key Laboratory of High Performance Ceramics and Superfine Microstructure, Shanghai Institute of Ceramics, Chinese Academy of Sciences, 1295 Dingxi Road, Shanghai 200050, People's Republic of China

Received May 15, 2006; E-mail: liangaoc@online.sh.cn

Controlled synthesis of inorganic nanoparticles (NPs) has become one of the important topics of colloid and materials chemistry because of their size- or shape-dependent properties and their potentials of self-assembly as building blocks—artificial atoms for diverse superstructures and mesocrystals.[1] The deep understanding of the nucleation and growth processes enables us to control the shape and size of NPs better.[2] As one of the most reactive rare earth materials, ceria (cerium oxide, CeO_2) has attracted a great deal of attention due to its unique applications in conversion catalysts, three-way catalysts (TWCs), fuel cells, solar cells, gates for metal-oxide semiconductor devices and phosphors.[3] Experimental[4] and theoretical[5] studies have shown surface structure-dependent reactivity of ceria nanocrystallites, and the (100) terminated surface is more reactive and catalytically important than (111) and (110) surfaces. In particular, the (100) surface is a "type III" surface, and there is a dipole moment perpendicular to the surface, which means its surface energy diverges and the structure is considered less stable.[6] Therefore, shape-controlled synthesis of ceria NPs with various morphologies (e.g., polyhedron-, tadpole-, wire-, rod-, and tube-like) is of potentially significant importance.[7]

Here we report shape- and size-controlled synthesis of ceria nanocubes bounded by six {200} planes through a rational one-pot approach[8] and their two-dimensional (2D) and 3D self-assembly on substrate. Both shape and size of the ceria NPs could be tuned more conveniently by changing the concentration of the reactants, the amount of stabilizing agents (especially for oleic acid (OLA)), and the water/toluene ratio in the reaction system. More importantly, due to the presence of oriented aggregation mediated precursor growth, the synthesized ceria nanocubes exhibit fantastic structural properties (rough {200} surfaces), which are extremely intriguing for their catalytic applications.[4a] Slow evaporation of the particle dispersion also yields NP arrays with 2D and 3D assembled patterns.

Figure 1 shows the morphological and structural properties of the ceria NPs. At the low concentration of $Ce(NO_3)_3$ in the water phase (16.7 mmol/L), monodisperse nanocubes with the average size of 4.43 ± 0.82 nm are formed (Figure 1a). The selection area electron diffraction (SAED) pattern reveals that all the detectable rings are perfectly indexed to the same positions as those from cubic fluorite structured ceria, and the (200) diffraction ring has an enhanced brightness. The high-resolution TEM (HRTEM) image shows the dominant {200} lattice fringes. At the high concentration of Ce(III) in the water phase (50.0 mmol/L), the gained nanocubes apparently have a bimodal size distribution and they could be easily separated from the crude solution by a two-step precipitation operation.[8] The small-sized nanocubes always have an average size of ~4 nm, while the size of large-sized nanocubes can be controlled by tuning the ratio of OLA/Ce(III), and the size increases with the increase of the OLA/Ce(III) molar ratio. Figure 1b,c shows the TEM image of the 7.76 ± 1.01 and 15.65 ± 2.06 nm nanocubes derived from the OLA/Ce(III) ratio of 6 and 8, respectively; further increasing the ratio to 10 results in cubic mesocrystals with the sizes of ~50−100 nm.[8] Careful examination of the large-sized nanocubes reveals that there are pits in them, and the surfaces are rough. The nanocubes have a strong tendency to assemble into 2D arrays with a regular pattern on the TEM grid with an increase of the sizes (Figure 1b,c). Figure 1c is recorded after tilting the sample by an angle of 20°, and a cubic shape of the sample can be clearly seen.

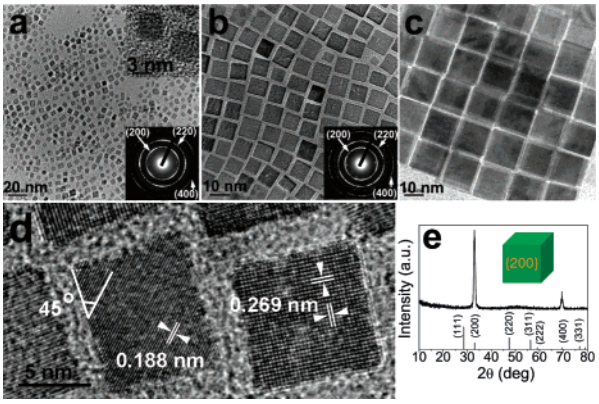

Figure 1. (a−c) TEM images of ceria nanocubes with the average sizes of (a) 4.43 nm, (b) 7.76 nm, and (c) 15.65 nm; the insets are SAED patterns and individual NPs. (d) HRTEM image of the ceria nanocubes. (e) A typical XRD pattern of the ceria nanocubes assembled on a Si wafer; the inset is the schematic illustration of the facets of an individual cube.

The facets of the synthesized cubic ceria NPs can also be determined by HRTEM, operated by directing the incident electron beam perpendicular to the square facet of the cube. The interfringe distances of the dominant 2D lattice fringes of the HRTEM image are 0.269 nm, close to the {200} lattice spacing of the cubic phase of ceria at 0.271 nm. Furthermore, the perpendicular {200} lattice fringes are either parallel to or orthogonal to the edge of the cube, and the occasionally observed {220} fringes (spacing 0.191 nm) run face-diagonally in the cube (Figure 1d; this can be further confirmed by the TEM tilted angle analysis). Therefore, the six surfaces of the nanocube are terminated with {200} planes.

Compared with the OLA tails interdigitating at ~2.2 nm, the shorter interparticle spacing of ~1.3−1.9 nm in the regular arrays (Figure 1b,c) excludes a simple surfactant-mediated self-assembly. The large-sized nanocubes (e.g., 15.65 nm) can also self-assemble into 3D NP arrays through the evaporation of a mixed solvent of toluene and ethanol.[8] The strong dipole−dipole interactions from the polar {200} surfaces are probably the driving force for self-assembly of the nanocubes because long-range van der Waals forces become difficult to control for NPs whose dimensions are beyond molecular length scales ($d > 10$ nm).[9] Figure 1e shows a typical XRD pattern recorded from the sample assembled on the single-crystalline Si wafer. The peaks are assigned to the diffraction of (200) and (400) planes of the cubic phase of ceria only ($Fm3m$, $a = 5.41134$ Å, JCPDS Card No. 34-0394), and other peaks corresponding to (111), (220), (311), (222), and (331) diffraction

10.1021/ja063359h CCC: $33.50

Scheme 1. Schematic Representation of the Oriented Aggregation Mediated Precursor Growth Mechanism of Colloidal NPs

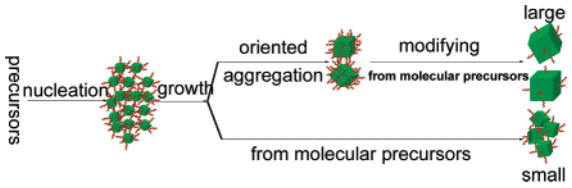

are not observed, indicating that only the (200) [and (400)] planes have a chance to be diffracted. This further confirms that the nanocubes assembled on the surface of the Si wafer are perfect cubes as schemed and also implies that {200}-perfect-oriented monolayers or thickness-controlled films composed of ceria nanocubes could be achieved from the present method.

The small-sized nanocubes (e.g., 4.43 nm) should be formed through the much faster growth of {111} planes than the {200} planes of the cubic phase of ceria[10] by the selective adsorption of oleic acid molecules on the {200} surfaces.[11] The relatively low molar ratio of OLA/Ce(III) yields a mixture of polyhedral and cubic NPs with the average size of 3.12 ± 0.40 nm.[8]

Interestingly, the large-sized nanocubes are believed to be formed through the oriented aggregation mediated precursor growth, which means nucleation—aggregation (with surfactant molecules pealing off)—growth (from molecular precursors) (Scheme 1). It should be noted that there exist a few (~0.1%) large-sized nanocubes with the sizes of 12−17 nm in the sample of 4.43 nm nanocubes.[8] HRTEM images and the corresponding FFT patterns show the single-crystalline nature of these nanocubes, but the presence of displacements, dislocations, domains, and the rough surfaces in these single-crystalline nanocubes imply that they come from the aggregation growth of crystal nuclei. With an increase of Ce(III) concentration, the amount of large-sized nanocubes in the whole reaction system increases and their sizes exhibit a typical bimodal distribution. In addition, it seems that the reduction of the water/toluene ratio (which means the insufficiency of continued precursors) could indicate the misorientation for the formation of the large-sized nanocubes because of the insufficiency of the modifying growth from molecular precursors. Large-sized and small-sized NPs coexist in the whole reaction system in this situation, whereas the large-sized nanocubes could not be further smoothed at the cost of the small particles. This implies that the current system may be absent of Ostwald ripening because of the low solubility of the OLA-capped ceria in the water phase. The intermediate NPs could be seen with a shortened reaction time.[8] Moreover, increasing the initial Ce(III) concentration in the water phase (which means increased supersaturation and decreased OLA/Ce(III) ratio) results in flowery NPs, and these misorientations directly reflect the oriented attachment process of small NPs.[12] The flowery NPs are formed by epitaxially attaching and fusing imperfectly cubic (mostly polyhedral) crystal nuclei (derived from the relatively decreased OLA/Ce(III) ratio) on (200) surfaces to reduce surface free energy through the removal of the (200) high-energy surfaces with the surfactant molecules pealing off.[13]

Usually, the exposure of crystallographically uniform facets of the cubic nuclei (only {200} planes) can favor their perfect oriented attachment with surfactant molecules pealing off, and they can form symmetrical cubic morphology to reduce the overall surface energy of the system. Sometimes, rod-like ceria can also be prepared in the present reaction system at varied conditions.[8] These highly anisotropic NPs may come from oriented attachment mediated precursor growth of crystal nuclei (or primary NPs) driven by the dipole−dipole interaction of polar {200} surfaces, as the formation of II(IV)−VI semiconductor nanowires or nanorods by an oriented attachment mechanism.[14] It should be noted that the present nanorods are always along [100] and enclosed by {200} planes, which is different from the previous reports.[4b,c,7c]

The perfect large-sized ceria nanocubes result from the perfect oriented aggregation of primary NPs followed by growth from the molecular precursors. This is extremely important for crystallization science and morphosynthesis. It will open up new avenues for the controlled synthesis of NPs with desirable properties, such as the incorporation of a heterogeneous atom or NP for semiconductor NP doping or a heterogeneous (e.g., core/shell) nanostructure. In view of the unique properties of {200} surfaces for ceria, the synthesized nanocubes should be of importance for both theoretical investigations and technological applications.

Acknowledgment. This work was financially supported by the National Basic Research Program (2005CB623605) and Shanghai Nanotechnology Promotion Center (0552nm045).

Supporting Information Available: Detailed preparation procedures, TEM, HRTEM images, and the Fourier analysis. This material is available free of charge via the Internet at http://pubs.acs.org.

References

(1) (a) Law, M.; Sirbuly, D. J.; Johnson, J. C.; Goldberger, J.; Saykally, R. J.; Yang, P. D. *Science* **2004**, *305*, 1269. (b) Shevchenko, E. V.; Talapin, D. V.; Murray, C. B.; O'Brien, S. *J. Am. Chem. Soc.* **2006**, *128*, 3620. (c) Cölfen, H.; Antonietti, M. *Angew. Chem., Int. Ed.* **2005**, *44*, 5576.
(2) (a) Shevchenko, E. V.; Talapin, D. V.; Schnablegger, H.; Kornowski, A.; Festin, O.; Svedlindh, P.; Haase, M.; Weller, H. *J. Am. Chem. Soc.* **2003**, *125*, 9090. (b) Cölfen, H.; Mann, S. *Angew. Chem., Int. Ed.* **2003**, *42*, 2350.
(3) (a) Fu, Q.; Saltsburg, H.; Flytzani-Stephanopoulos, M. *Science* **2003**, *301*, 935. (b) Trovarelli, A. *Catal. Rev. Sci. Eng.* **1996**, *38*, 439. (c) Murray, E. P.; Tsai, T.; Barnett, S. A. *Nature* **1999**, *400*, 649. (d) Corma, A.; Atienzar, P.; Garcia, H.; Chane-Ching, J. Y. *Nat. Mater.* **2004**, *3*, 394. (e) Tye, L.; El-Masry, N. A.; Chikyowm, T.; McLarty, P.; Bedair, S. M. *Appl. Phys. Lett.* **1994**, *65*, 3081. (f) Morshed, A. H.; Moussa, M. E.; Bedair, S. M.; Leonard, R.; Liu, S. X.; ElMasry, N. *Appl. Phys. Lett.* **1997**, *70*, 1647.
(4) (a) Aneggi, E.; Llorca, J.; Boaro, M.; Trovarelli, A. *J. Catal.* **2005**, *234*, 88. (b) Zhou, K.; Wang, X.; Sun, X.; Peng, Q.; Li, Y. *J. Catal.* **2005**, *229*, 206. (c) Mai, H.-X.; Sun, L.-D.; Zhang, Y.-W.; Si, R.; Feng, W.; Zhang, H.-P.; Liu, H.-C.; Yan, C.-H. *J. Phys. Chem. B* **2005**, *109*, 24380.
(5) (a) Sayle, D. C.; Maicaneanu, S. A.; Watson, G. W. *J. Am. Chem. Soc.* **2002**, *124*, 11429. (b) Herman, G. S. *Surf. Sci.* **1999**, *437*, 207. (c) Skorodumova, N. V.; Baudin, M.; Hermansson, K. *Phys. Rev. B* **2004**, *69*, 075401.
(6) (a) Tasker, P. W. *J. Phys. C* **1979**, *12*, 4977. (b) Conesa, J. C. *Surf. Sci.* **1995**, *339*, 337.
(7) (a) Wang, Z. L.; Feng, X. *J. Phys. Chem. B* **2003**, *107*, 13563. (b) Yu, T.; Joo, J.; Park, Y. I.; Hyeon, T. *Angew. Chem., Int. Ed.* **2005**, *44*, 7411. (c) Vantomme, A.; Yuan, Z.-Y.; Du, G; Su, B.-L. *Langmuir* **2005**, *21*, 1132. (d) Han, W.-Q.; Wu, L.; Zhu, Y. *J. Am. Chem. Soc.* **2005**, *127*, 12814.
(8) See the Supporting Information.
(9) Wei, A. *Chem. Commun.* **2006**, 1581.
(10) (a) Wang, Z. L. *J. Phys. Chem. B* **2000**, *104*, 1153. (b) Sun, Y.; Xia, Y. *Science* **2002**, *298*, 2176.
(11) Stubenrauch, J.; Brosha, E.; Vohs, J. M. *Catal. Today* **1996**, *28*, 431.
(12) (a) Penn, R. L.; Banfield, J. F. *Science* **1998**, *281*, 969. (b) Banfield, J. F.; Welch, S. A.; Zhang, H.; Ebert, T. T.; Penn, R. L. *Science* **2000**, *289*, 751. (c) Lee, W.-H.; Shen, P. *J. Cryst. Growth* **1999**, *205*, 169.
(13) Alivisatos, A. P. *Science* **2000**, *289*, 736.
(14) (a) Tang, Z.; Kotov, N. A.; Giersig, M. *Science* **2002**, *297*, 237. (b) Cho, K.-S.; Talapin, D. V.; Gaschier, W.; Murray, C. B. *J. Am. Chem. Soc.* **2005**, *127*, 7140. (c) Yu, J. H.; Joo, J.; Park, H. M.; Baik, S.-I.; Kim, Y. W.; Kim, S. C.; Hyeon, T. *J. Am. Chem. Soc.* **2005**, *127*, 5662.

JA063359H